Available online at www.sciencedirect.com
ScienceDirect

Signal Processing: *Image Communication* 22 (2007) 543–556

SIGNAL PROCESSING: IMAGE COMMUNICATION

www.elsevier.com/locate/image

A robust joint source channel coding scheme for image transmission over the ionospheric channel

C. Chatellier[a,*], H. Boeglen[b], C. Perrine[a], C. Olivier[a], O. Haeberlé[b]

[a]*SIC Laboratory, EA CNRS 4103, Bvd Marie et Pierre Curie, F-86962 Futuroscope Chasseneuil Cedex, France*
[b]*MIPS Laboratory 12, rue des frères Lumière 68093-Mulhouse, Cedex, France*

Received 24 October 2006; received in revised form 9 May 2007; accepted 9 May 2007

Abstract

In this paper, we propose a joint source channel coding (JSCC) scheme to the transmission of fixed images for wireless communication applications. The ionospheric channel which presents some characteristics identical to those found on mobile radio channels, like fading, multipath and Doppler effect is our test channel. As this method based on a wavelet transform, a self-organising map (SOM) vector quantization (VQ) optimally mapped on a QAM digital modulation and an unequal error protection (UEP) strategy, this method is particularly well adapted to low bit-rate applications. The compression process consists in applying a SOM VQ on the discrete wavelet transform coefficients and computing several codebooks depending on the sub-images preserved. An UEP is achieved with a correcting code applied on the most significant data. The JSCC consists of an optimal mapping of the VQ codebook vectors on a high spectral efficiency digital modulation. This feature allows preserving the topological organization of the codebook along the transmission chain while keeping a reduced complexity system. This method applied on grey level images can be used for colour images as well. Several tests of transmission for different images have shown the robustness of this method even for high bit error rate (BER $> 10^{-2}$). In order to qualify the quality of the image after transmission, we use a PSNR% (peak signal-to-noise ratio) parameter which is the value of the difference of the PSNR after compression at the transmitter and after reception at the receiver. This parameter clearly shows that 95% of the PSNR is preserved when the BER is less than 10^{-2}.

Keywords: Image coding; Joint source channel coding; Discrete wavelet transform; Image transmission over noisy channel

1. Introduction

Nowadays, there is a constant increase in services offered by mobile phone providers. The quantity and diversity of information to be transmitted requires increasingly complex coding and transmission technologies. The constraints linked to mobility are very important. Their consequences, such as fading, Doppler effect and spreading delay, produce transmission errors, which can have a dramatic impact on the quality of the signal content. The currently available channel coding and decoding methods linked to equalization, allow the correction of most of these errors, thereby guaranteeing a good quality of service. However, the use of these techniques results in an increase of the quantity of data to be transmitted. This results in an increase of the transmission time if the bit rate is constant, or

*Corresponding author. Tel.: +33 5 49 49 74 39; fax: +33 5 49 49 65 70.
E-mail address: chatellier@sic.univ-poitiers.fr (C. Chatellier).

0923-5965/$ - see front matter © 2007 Elsevier B.V. All rights reserved.
doi:10.1016/j.image.2007.05.001

of the bandwidth for variable bit rate. In this context, image compression algorithms represent a useful alternative since they allow the reduction in size of the transmitted files, whilst ensuring an excellent visual quality.

Amongst all these image coding methods, discrete cosine transform (DCT) and discrete wavelet transform (DWT) are widely used. Their usefulness comes from their capability to compress information to a relatively small number of coefficients and, of course, from their reversibility. When the compression rate is high, there are different types of distortion or artefacts depending on the compression methods. JPEG [24], which is based on DCT, suffers from blocking artefacts. JPEG-2000 [14], SPIHT [12] and EBCOT [6] which are based on DWT suffer from ringing around edges.

Unfortunately compressed images are very sensitive to transmission errors and this sensitivity increases with the compression rate. Fig. 1 below shows the impact of these errors on the quality of a reconstructed image with a bit error rate (BER) in the order of 10^{-4}. This results from the arithmetic coding used at the last compression algorithm stage, necessary for the binary coding of quantized coefficients. Due to this variable length coding (VLC) any error occurring in the bit stream results in a desynchronisation of the decoding algorithm. In most cases, this produces an increasing series of errors, preventing image reconstruction [26].

In order to counteract this phenomenon, marks are introduced in the compression process, which allow the synchronisation of the decoding process for these VLC when transmission errors occur [5,11,28]. Fig. 2 shows the image resulting from the introduction of such marks in a JPEG image. However, as the BER increases so does the number of required marks resulting in a strongly degraded image.

Channel coding or error correcting codes (ECC), which aims at detecting and correcting transmission errors, can also be introduced. The correcting capability of these codes is linked to the redundancy introduced in the transmitted bit stream. Their performance has been widely demonstrated. In order to achieve an efficient image transmission

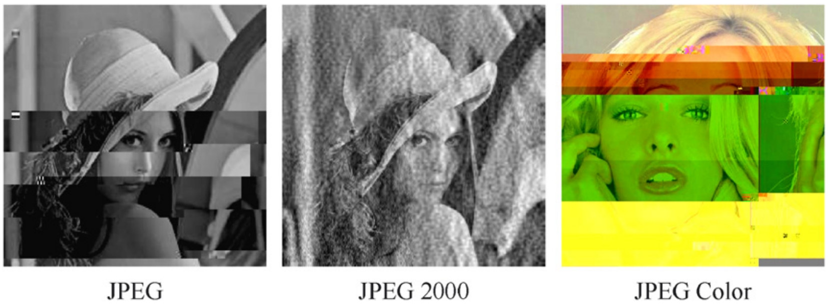

Fig. 1. Images reconstruction when BER is about 10^{-4} and file header not corrupted.

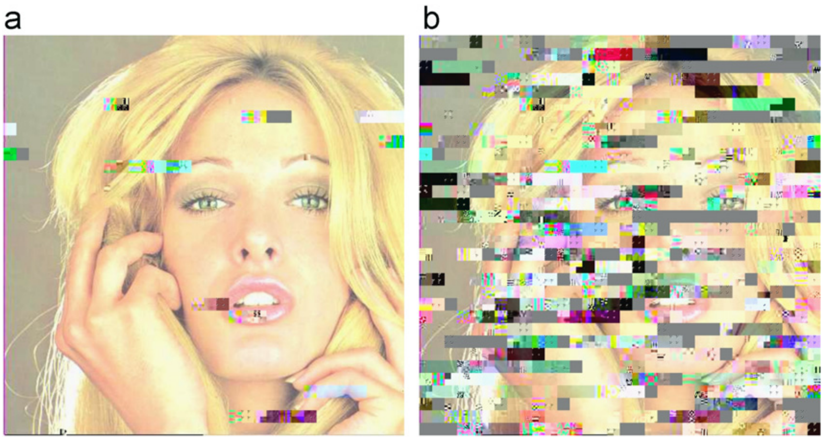

Fig. 2. Resynchronised binary stream for a JPEG image: (a) BER = 10^{-4}, (b) BER = 4.12×10^{-3}.

scheme when BER is very high, most solutions proposed in the literature are based on concatenated ECC and unequal error protection (UEP). For example, [27] proposes a system that reorganizes the JPEG 2000 stream and protects it with a Reed–Solomon (RS) and a Turbo Code. In [7] a concatenated cyclic redundancy Check code (CRC)/ rate compatible punctured convolutional code (RCPC) associated with an RS code allows an efficient error protection of images during transmission. In [20] a combination of forward error correction (FEC) with a zerotree wavelet packetization method allows having high performance in transmission. Generally, the improvement of the robustness of an image transmission system generates two effects. The first one is a global increase of the receiver's complexity and the second one is a decrease of the bit-rate devoted to image information transmission. The latter is directly linked to the ECC rate. In fact, an efficient compressed image transmission system using JPEG, SPIHT or JPEG2000 generally requires a code rate less than 0.4. This means that 60% of the transmitted data is devoted to error protection. In our context of low transmission bit-rate (8 kb/s) and high BER ($>10^{-2}$), this proportion is inapplicable. This is the reason why our work does not use the classical compression algorithms (JPEG, JPEG2000, SPIHT) but presents a new image transmission scheme suitable for ionospheric channels, which uses an association between vector quantization (VQ) techniques, DWT and digital modulations. This paper is organized as follows: Section 2 defines the experimental context and the radio link quality on which images must be transmitted. Section 3 is devoted to a JSCC strategy in order to achieve a reduced complexity system. Firstly, we present an error resilient VQ scheme based on Kohonen's self-organizing map (SOM) algorithm. JSCC is achieved by mapping the obtained codebook on a high spectral efficiency digital modulation. Secondly, we specify our wavelet transform self-organizing map (WTSOM) algorithm, which improves significantly the compression rate while keeping the previous JSCC strategy. Simulation and experimental results are given in Sections 4 and 5, respectively.

2. Transmission context

Transmission d'Images par Liaison IONisphérique (TRILION) is a French acronym for 'image transmission over the ionosphere'. Its goal is to establish a relatively wide bandwidth link in the high frequency (HF) band in order to reach a high transmission rate. This project involves two entities: the Institute of Electronics and Telecommunications (IETR) and the Signal Image Communication (SIC) laboratories from the University of Rennes and Poitiers, respectively.

2.1. The ionospheric channel

HF waves (3–30 MHz), when propagated through the ionosphere, can reach very long distances with a minimal infrastructure compared to satellite links, for example. In order to understand why the ionospheric channel is noisy, it is necessary to start with a short description of ionospheric propagation and its effects on transmission. Two main phenomena must be considered. The first one is that waves can follow several distinct paths by reflecting themselves against different layers of the ionosphere. Then, the transmitted signal generates many replicas, which are affected in different ways by the channel: their differential time delays can be large, their Doppler shifts and angles of arrival can be spaced out too. The second phenomenon appears because of Earth's magnetic field, which makes the medium anisotropic. Within each path, the wave splits into two complementary propagation modes called O (ordinary) and X (extraordinary). Both are very close and, therefore, have similar time delays, Doppler shifts and direction of arrivals (DOA's). On the other hand, their polarization properties are very different. In the plane orthogonal to the direction of propagation, their electromagnetic fields describe orthogonal ellipses clockwise or counter clockwise [18]. These two phenomena explain why the ionospheric channel is both multipath, as shown in Fig. 3, and multimode, and this fact strongly degrades the signal-to-noise ratio (SNR). Studies have shown [17] that the capacity of ionospheric channels is in the order of 2 bits/s/Hz, thus yielding a maximum transfer rate of 8 kb/s when using a 16-QAM modulation.

2.2. Effects on transmission

The transmitted signal replicas created by multipath and multimode propagation degrade the transmission quality. Two phenomena of the same nature but with different consequences can occur. For example, if two signals are delayed by an interval less than $1/B$ (where B is their bandwidth),

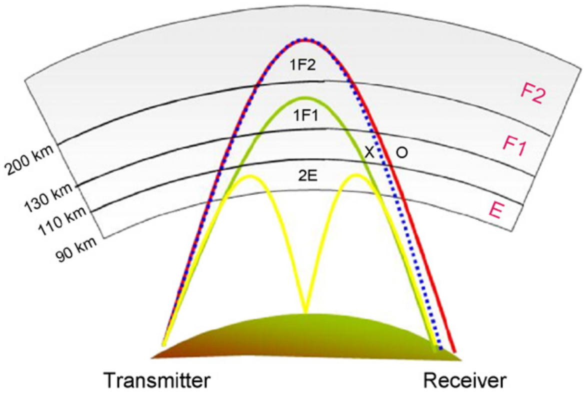

Fig. 3. Multipath and multimode propagation in the ionosphere.

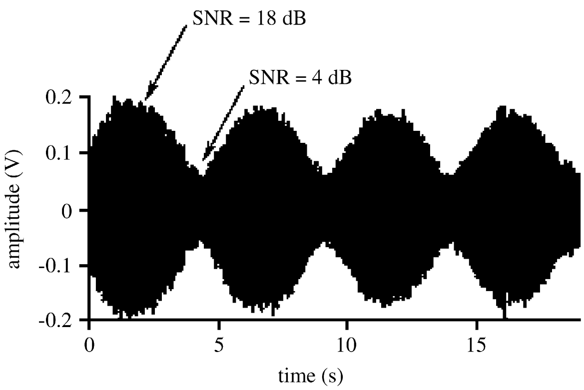

Fig. 4. Example of a fading signal, carrier frequency of 8 MHz 16-QAM modulation and 3 kHz bandwidth.

then the resultant signal will fade, making the SNR variable in time, as shown in Fig. 4.

The link used for this experiment has been established in France between Poitiers (lat.: 46°31′N, long.: 0°25′E) and Monterfil (lat.: 48°03′N, long.: 2°00′W) near Rennes and is about 300 km long. The complete transmitting system has already been described in a previous paper [22]. The transmitter is located in Poitiers and is composed of a computer, a complex modulator and a single delta antenna. The receiving system, located in Monterfil, is a set of eight collocated active antennas described in [19].

2.3. Experimental BER results

Several tests have been performed using a 16-QAM modulation, a symbol duration of 0.4 ms and carrier frequencies ranging from 6 to 9 MHz. During these tests, 72 files were transmitted and for many reasons, some of them were unusable

Table 1
BER results for different files transmitted over the ionospheric channel

Carrier frequency	BER interval	Number of files
6994 MHz (27 files)	$0 \leqslant \mathrm{BER} \leqslant 10^{-4}$	21
	$10^{-4} < \mathrm{BER} \leqslant 10^{-3}$	0
	$10^{-3} < \mathrm{BER} \leqslant 10^{-2}$	0
	$\mathrm{BER} > 10^{-2}$	6
7967 MHz (22 files)	$0 \leqslant \mathrm{BER} \leqslant 10^{-4}$	2
	$10^{-4} < \mathrm{BER} \leqslant 10^{-3}$	16
	$10^{-3} < \mathrm{BER} \leqslant 10^{-2}$	3
	$\mathrm{BER} > 10^{-2}$	1
8917 MHz (8 files)	$0 \leqslant \mathrm{BER} \leqslant 1.10^{-4}$	0
	$10^{-4} < \mathrm{BER} \leqslant 10^{-3}$	5
	$10^{-3} < \mathrm{BER} \leqslant 10^{-2}$	3
	$\mathrm{BER} > 10^{-2}$	0

(received signal too weak due to bad propagation conditions, jamming, pulse noise too high, etc.). The number of useable files was 57 and the size of each file was 11 kbytes. Table 1 gives an exhaustive list of the results detailed in [8].

The results show clearly that it is very difficult to estimate the BER in this type of transmission. Conditions of signal propagation are indeed linked with solar activity, which varies according to the time of day, date, season, year and to the carrier frequency that has been used to transmit the signal. According to the results, BER can range from 0 to 10^{-2}, which means that it is impossible to transmit JPEG images without a sophisticated ECC scheme. These difficulties have resulted in the development of a new JSCC strategy described in the next section.

3. Joint source channel coding

The aim of joint source channel coding is to increase the robustness of the transmission chain by reducing the impact of errors on the quality of the reconstructed image while keeping the system as simple as possible. In the TRILION configuration, we first used SOM VQ whose codebook was optimally mapped on high spectral efficiency modulations. Finally the new coding scheme called WTSOM was introduced.

3.1. SOM VQ JSCC

The first joint source channel coding strategy involved SOM VQ in combination with high spectral efficiency modulation mapping. There are many efficient VQ algorithms in the literature (LBG, K-Means), but none, except SOM has error resilience properties [21]. These notions are detailed below.

3.1.1. Compression by VQ

There are two main lossy compression approaches. The transform methods are such as JPEG, JPEG2000, EBCOT and SPIHT [6,12,14,24] which are very well-known, and VQ [1]. In order to obtain a more efficiently coded representation of image data, the first stage of a compression scheme is image decomposition or transformation. The second stage deals with quantization in order to reduce the amount of data: it is the lossy stage. Finally, the third stage is a binary symbol encoding. In this part we focus on the VQ technique which is very useful in JSCC. VQ is a clustering method, grouping similar vectors into one class. The vectors are obtained from the image data by extracting non-overlapping square blocks of size $n \times n$. Each vector is then compared to a set of vectors from a codebook. The best-matched code vector is then chosen using a distortion rule. The encoder generates the address of the coded vector (smaller in size than the coded vector) and sends it to the receiver. The decoder uses this address to generate the code vector from the same codebook and to reconstruct the image [15]. The most widely used distortion measure is the squared Euclidean distance between the input vector $c_i = [c_1, c_2, \ldots, c_l]^{\mathrm{T}}$ and the output $\hat{c}_i = [\hat{c}_{i1}, \hat{c}_{i2}, \ldots, \hat{c}_{il}]^{\mathrm{T}}$ given by

$$d(c_i, \hat{c}_i) = \sum_{k=1}^{l} (c_k - \hat{c}_{ik})^2 = ||c - \hat{c}_i||^2. \quad (1)$$

In this way, the approximation of the original image is obtained with a minimum distortion ratio. The transmission scheme is depicted in Fig. 5.

Among the different approaches currently used to design a codebook [3,23,25], we have chosen the SOM method proposed by Kohonen [3]. Thanks to the topological organization of the obtained codebook, this algorithm has an interesting error resilience property as will be shown in the next section. From a set of 15 512×512 pixel images and a square block size of 3×3 pixels, we obtain an organized codebook as shown in Fig. 6(a). This codebook contains 256 data vectors of 9 pixels. Applying this VQ on the "Fruits" image results in Fig. 6(b). The visual quality is very good and the PSNR is 27.93 dB. A detail outlined in Fig. 6(c) shows clearly the block effect due to the quantization step.

The compression rate depends on the number and the size of the vectors in the codebook. Choosing a codebook of size (M) and vectors of size (N), for 8 bits/pixel images, the compression rate can be calculated by

$$R = 8N/\log 2M. \quad (2)$$

So, for a 256-vector codebook and a grey scale image, the compression rate will depend only on the vector size (N). If the square block size $N = n \times n = 9$ then $R = 9$. The next section will deal with the transmission of these SOM coded images.

3.1.2. SOM VQ mapping

In [13] Pyndiah proposed a JSCC based on the mapping of a 256-vector codebook on a 256-QAM modulation. This high spectral efficiency modulation is defined by the number M of symbols which is

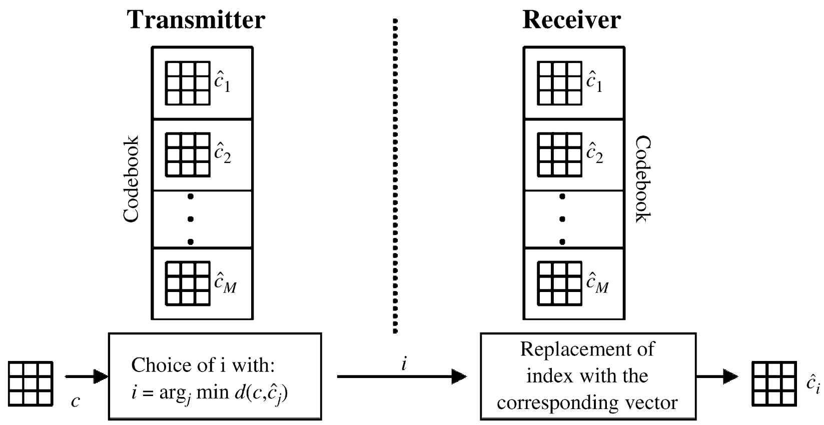

Fig. 5. Configuration of the transmitter and receiver for a transmission in VQ case.

Fig. 6. Result of VQ applied on fruit image, PSNR = 27.93 dB. (a) Codebook, (b) reconstructed image, (c) block effect due to the quantization.

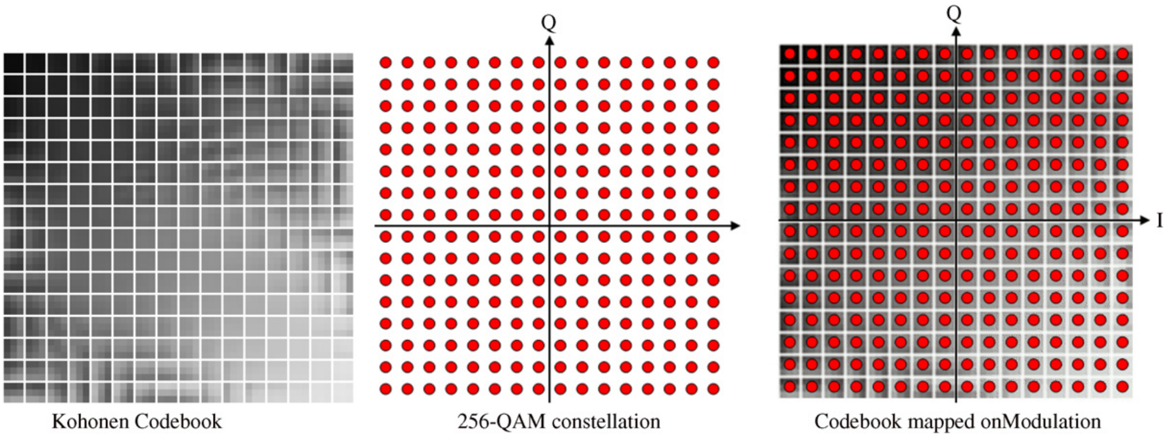

Fig. 7. Mapping of the SOM codebook on a 256-QAM modulation.

chosen according to a compromise between the desired bit rate, the available bandwidth and the quality of the radio link. When the number of symbols M equals the number of vectors, it is possible to map the codebook vectors on the constellation symbols thus keeping the codebook organisation along the transmission chain as shown in Fig. 7.

In this configuration, a wrong symbol detected produces a decoded vector very similar to the original one since the Euclidean distance between them is very close. Some results are shown in Fig. 8, where a 256-QAM modulation has been used on an AWGN channel. The SNR is equal to 16 dB ($\text{BER} = 1.3 \times 10^{-2}$) and 13 dB ($\text{BER} = 4.1 \times 10^{-2}$). The visual quality of the images highlights the robustness of this method.

When the SNR of a radio link is too low, thus yielding high BER values, high spectral efficiency modulations cannot be used. In order to minimize the BER one can decrease the number of bits per symbol and use a 64-QAM (or 16) modulation. In these cases the optimal mapping of a 256 bytes codebook is no longer possible. In order to solve this problem, Pyndiah [13] suggests reorganising the codebook differently. In the case of 16-QAM modulation, for example, the SOM algorithm is trained in order to obtain a four-dimension codebook ($4 \times 4 \times 4 \times 4$) suitable for 4 bits 16-QAM symbols. The results are not as good (1.5 dB loss in PSNR) as in the 256-QAM case but the system remains quite robust.

From what has been presented before, we can conclude that the joint optimization of SOM VQ and QAM modulation by appropriate mapping represents a good alternative to complex and bandwidth consuming ECC schemes on high BER channels. In order to increase the compression rate, we propose a new method adapted to these channels, detailed in the next section.

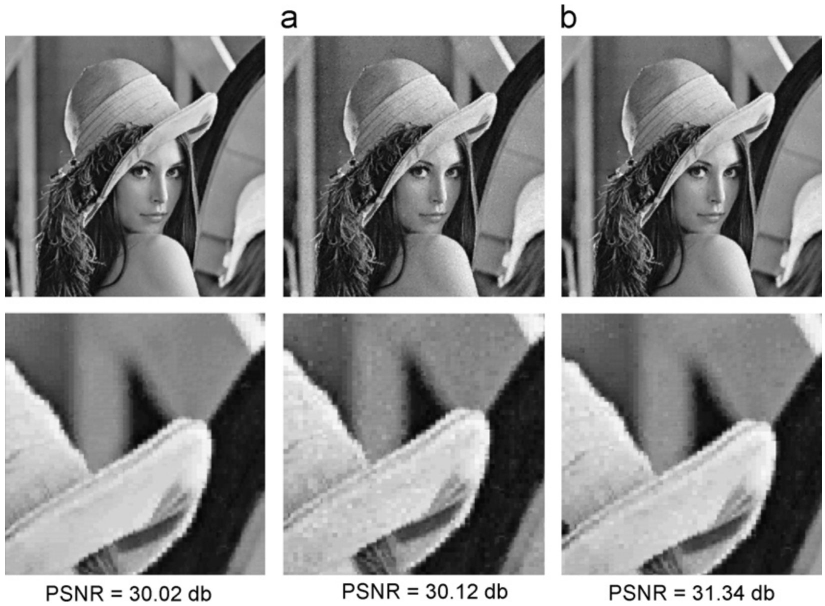

Fig. 8. QV-compressed image transmission over the AWGN channel and a 256-QAM modulation. (a) SNR $= E_b/N_o = 13$dB, (b) SNR $= E_b/N_o = 16$dB.

3.2. WTSOM JSCC

The method comprises two steps. Firstly, in order to increase the compression rate and obtain a hierarchical structure of the data, the compression stage is performed by a wavelet DWT similar to the one used in JPEG2000. Secondly, to maintain the robustness of the scheme a SOM VQ + an optimally QAM mapped strategy is applied on each sub-image of the DWT following the principles detailed in the previous section.

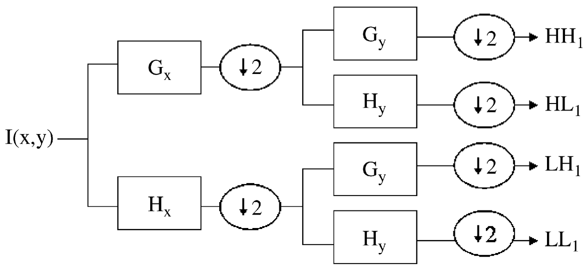

Fig. 9. Filter bank for wavelet decomposition of an image at the first scale ($\downarrow 2$ = decimation by 2).

3.2.1. First stage: image compression and DWT

A practical way of decomposing a signal into its wavelet coefficients is to apply a filter bank. Fig. 9 displays a 2-D case where $I(x, y)$ is the original image, G is a high-pass filter (applied along x then along y), H is a low-pass filter (applied along x then along y). H and G can be built so that they permit a perfect reconstruction of the original image. This first level of decomposition leads to:

- HH_1: sub-image of the diagonal details at scale 1.
- HL_1: sub-image of the vertical details at scale 1.
- LH_1: sub-image of the horizontal details at scale 1.
- LL_1: low-resolution sub-image at scale 1.

This filter bank can be re-applied n times to LL_1, to produce details and low-resolution sub-images at scale n. In our application, we use the Daubechies (9/7) biorthogonal wavelets (such as in the JPEG 2000 case) [10]: the coordinates in the wavelet series are computed with a different dual set of basis functions. These bases are not orthogonal, but they can be constructed to have temporal symmetry (filter). An example of wavelet decomposition at scale 2 is shown in Fig. 10.

A three-level wavelet decomposition of a 512×512 pixel image results in 10 sub-images which can be classified as follows:

Most significant data: LL_3. (64×64 coefficients).
Significant data: HL_3, LH_3, HH_3 (64×64 coefficients).
Medium significant data: HL_2, LH_2, HH_2. (128×128 coefficients).

Fig. 10. Wavelet decomposition of an image at scale 2.

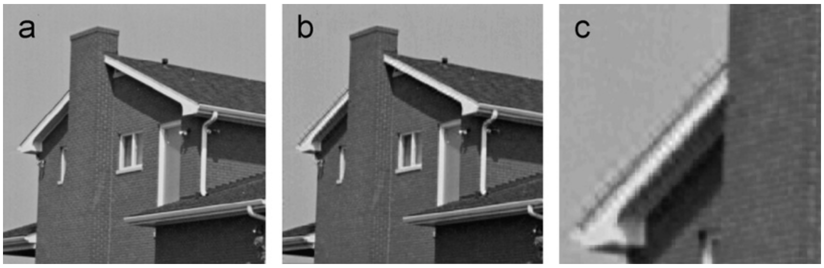

Fig. 11. House image rebuilt with coefficients LL_3, LH_3, HL_3, LH_2 and HL_2. (a) Original image; (b) rebuilt image: PSNR = 37.07dB, (0,3125bpp); (c) detail of image (b).

Lower significant data: HL_1, LH_1, HH_1. (256×256 coefficients).

In order to define the best compromise between the compression ratio and the visual quality of the image, we must select a restricted number of sub-images among the whole decomposition. After several visual tests, we decided to keep the following sub-images: LL_3, HL_3, LH_3, HL_2 and LH_2. This choice is justified by the visual quality of the image obtained although 83% of the data is discarded. An example is shown in Fig. 11 for the "House" image. The loss of quality is located on the edges and ringing artefacts appear but the visual quality remains acceptable for our application, which is dedicated to video conferences. Such images contain mostly low frequency coefficients and do not require a high-frequency description.

3.2.2. Second stage: image compression combining DWT and SOM algorithm

The idea we develop here consists in applying a specific SOM VQ on each preserved sub-image. In our application we have chosen the same size for each codebook. This choice allows comparing the efficiency of both methods (SOM and WTSOM) described in this article. As pointed out earlier we obtain five specific codebooks of 256 vectors whose size and structure (row, column or square) depends on the sub-image as described in Table 2.

The most significant coefficients are located in the sub-image LL_3 and are quantized with vectors of size 1×1. The sub-images HL_3 and LH_3 represent the horizontal and vertical details, respectively, hence, the choice of a column vector for the first one and a row vector for the second one. For the two last ones HL_2 and LH_2, details are less important than HL_3 and LH_3 and a square structure of size 4×4 is chosen. The sizes and the structures of these vectors result from a compromise between the compression ratio, the importance of the coefficients and the visual quality of the reconstructed image. The compression rate can be evaluated by the ratio between the number of bits of the original image and the number of bits transmitted. Table 3 summarizes these data and gives the appropriate values for the calculation of the compression ratio.

The compression ratio is adjustable according to the size of the vectors in each codebook. For instance, in order to obtain a lower compression rate one can choose smaller vectors for HL_2 and LH_2 as described in Table 4.

In this example, after VQ, the number of bits to transmit is 1,31,072 bits.

Table 2
Structure and size of vectors for each sub-image

Sub-image	LL_3	HL_3	LH_3	HL_2	LH_2
Number of coefficients	64×64	64×64	64×64	128×128	128×128
Size of vectors	1×1	2×1	1×2	4×4	4×4
Structure of vectors	□	□ □	□ □	□ □ □ □ □ □ □ □ □ □ □ □ □ □ □ □	□ □ □ □ □ □ □ □ □ □ □ □ □ □ □ □

Table 3
Codebook vector sizes for a compression rate of 25.6

Sub-image	LL_3	LH_3	HL_3	LH_2	HL_2	Total
Number of coefficients	64×64	64×64	64×64	128×128	128×128	45056
Size of vectors	1×1	1×2	2×1	4×4	4×4	
Number of vectors to transmit	$64 \times 64 = 4096$	$64 \times 64/2 = 2048$	$64 \times 64/2 = 2048$	$128 \times 128/16 = 1024$	$128 \times 128/16 = 1024$	10240
Number of vectors in the codebook	256	256	256	256	256	
Number of bits to transmit	4096×8	2048×8	2048×8	1024×8	1024×8	81920

Where the number of bits of the original image is: $512 \times 512 \times 8 = 2{,}097{,}152$ bits.
The number of bits to transmit is: 81,920 bits.
Then the compression ratio is: $T_c = 2{,}097{,}152/81{,}920 = 25.6$.
Which corresponds to 0.3125 bit per pixel.

Table 4
Codebook vector sizes for a compression rate of 16

Sub-image	LL_3	LH_3	HL_3	LH_2	HL_2	Total
Number of coefficients	64×64	64×64	64×64	128×128	128×128	45056
Size of vectors	1×1	1×2	2×1	2×2	2×2	
Number of vectors to transmit	$64 \times 64 = 4096$	$64 \times 64/2 = 2048$	$64 \times 64/2 = 2048$	$128 \times 128/4 = 4096$	$128 \times 128/4 = 4096$	16384
Number of vectors in the codebook	256	256	256	256	256	
Number of bits to transmit	4096×8	2048×8	2048×8	4096×8	4096×8	131072

And the compression rate $T_c = 2\,097\,152/131\,072 = 16$ (0.5 bpp).

In Table 5, the behaviour of the WTSOM algorithm is compared with the SOM algorithm for different values of the compression rate. As can be seen, in all cases, the WTSOM method yields better PSNR values than the SOM method. These results are always 8–10 dB worse than all others algorithms used in image compression processing like JPEG, SPIHT or JPEG 2000 for compression rates ranging from 0.3 to 0.8 bpp. However, as far as transmission is concerned, WTSOM allows to have better reconstruction capability when errors occur whilst being less complex and more bandwidth efficient.

The different steps of the transmission scheme are shown in Fig. 12.

In this section, we compared two methods using VQ and showed that WTSOM yields better results than SOM in terms of PSNR. The following section deals with the problem of WTSOM image transmission when the SNR is very low.

4. Image transmission in presence of errors

In order to compare the robustness of the two coding schemes (SOM and WTSOM), we performed an image transmission simulation on an AWGN channel using a 256-QAM modulation

Table 5
Comparison of PSNR for SOM and WTSOM coded images and different compression rates

Images	SOM $T_c = 9$	WTSOM $T_c = 9.14$	SOM $T_c = 16$	WTSOM $T_c = 16$	SOM $T_c = 25$	WTSOM $T_c = 25.6$
Desk	29.33	30.86	26.83	29.26	26.16	28.57
Einstein	32.79	37.71	29.79	34.04	28.80	32.57
Fruits	31.46	33.62	29.96	30.35	27.93	29.34
House	35.73	39.95	32.63	35.65	31.73	34.03
Lena	32.02	33.11	29.99	30.25	28.61	29.20

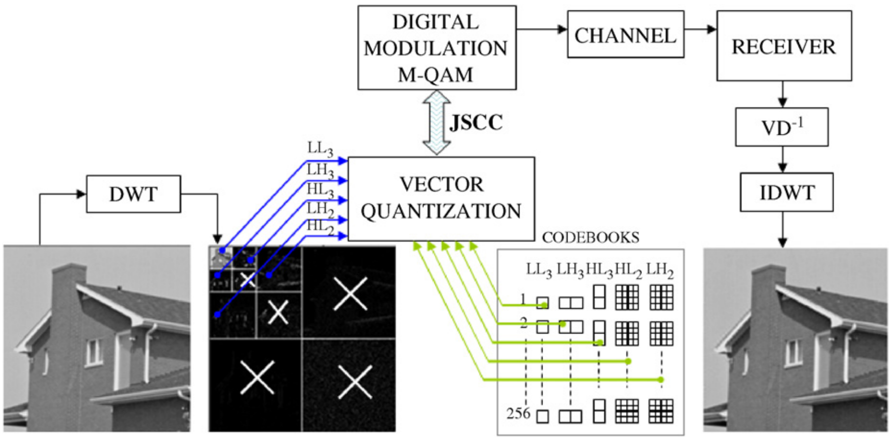

Fig. 12. Transmission chain including DWT, VQ and Modulation.

(see Fig. 13). From the visual analysis of the received images, an important feature can be pointed out. Although the number of visual errors in WTSOM scheme is less than in the SOM scheme, the visual impact is more important. In the WTSOM scheme, the visual impact of an error depends strongly on its location in the symbol stream. If an error affects the coarse image LL_3, which is the most important data, this error will propagate along all the reconstructed process and will appear very clearly on the reconstructed image. When an error affects the other sub-images, the visual impact is not as strong, as Fig. 14 shows.

In order to avoid these effects, it is obvious that the LL_3 sub-image needs a higher level of protection than the other sub-images. The hierarchical organization brought by DWT leads naturally to unequal error protection (UEP) strategies, which permit an efficient usage of channel bandwidth. Moreover, thanks to our jointly optimized SOM VQ+QAM modulation system we can expect a relatively high code rate to protect the most important data.

We have chosen to protect the LL_3 sub-image with an RS block code [16] because of its good correction capability and its practical interest. However, the code must not modify the organization between the codebook indices and the modulation symbols. It is thus necessary to respect the two following rules

(1) The systematic form of the code must be used in order to maintain the relation between the codebook vectors and the modulation symbols.
(2) The number of bits n and k of the code C (n, k, t) must be proportional to the number of bits used to represent the real and imaginary part of the modulation symbols.

The decoding of RS encoded blocks is performed using either hard or soft decoding. Soft decoding by means of the Chase algorithm [4] leads to an improvement, which can reach 2 dB at a BER of 10^{-5}.

Finally, the overall code rate of our system is in the order of 0.9 which is much higher than those used in the classical image transmission schemes as was pointed out in the beginning of this paper.

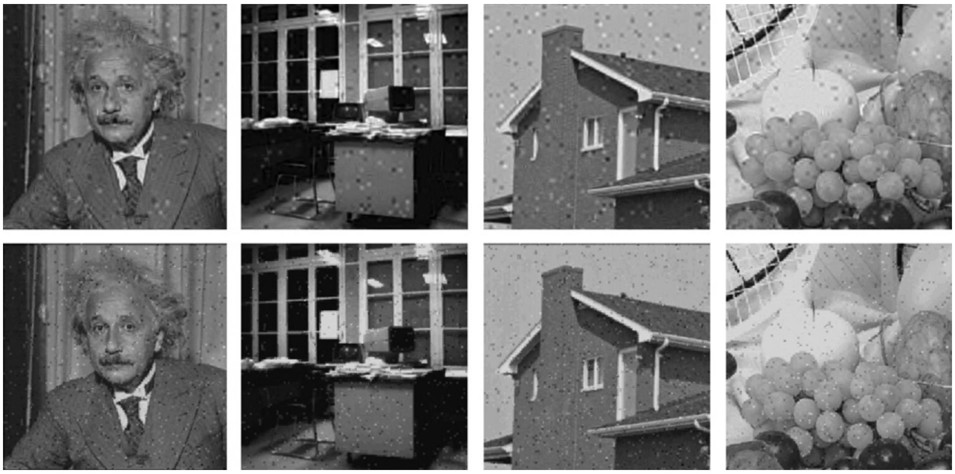

Fig. 13. Visual quality comparison for SOM and WTSOM received images: $T_c = 25.6$ (0.3125 bpp), 256-QAM modulation, $\text{BER} = 10^{-2}$.

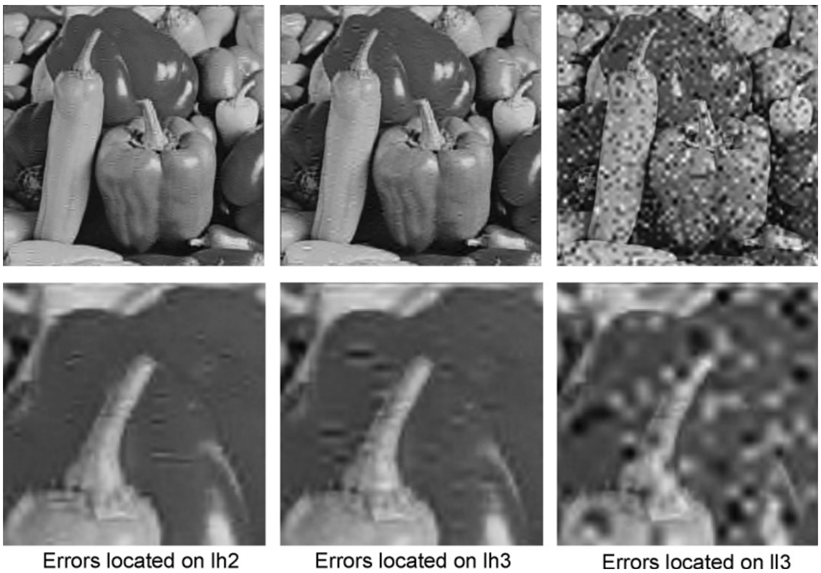

Fig. 14. Details of the visual impact of error transmission as a function of sub-band errors. Errors are located on a sub-image and $\text{BER} = 8 \times 10^{-2}$.

5. Experimental results

In this section, we are going to compare the performance of both JSCC schemes (SOM and WTSOM) when used with an ECC. For that purpose, the compression rates must be the same in both cases. In the first case (SOM), the protection of the data is achieved by an RS(255.227) code. Because of the added redundancy, the compression rate is decreased from 25.6 to 22.3. In the second case (WTSOM), the RS code must only protect the LL_3 sub-image data. In order to obtain the same compression rate than in the previous case, an RS(255.187) code is used. Three results are shown in Fig. 15. They have been obtained from a transmission on the operational radio link set up between Poitiers and Rennes described above (both in France, range of 300 km) using carrier frequencies in the 3–8 MHz band [2]. In this experiment, we transmitted, using an optimally mapped 16-QAM modulation [13], 20 kbits files each containing a 256×256 compressed image and its specific error protection using the techniques described before. The global compression rate was 25 (0.32 bpp).

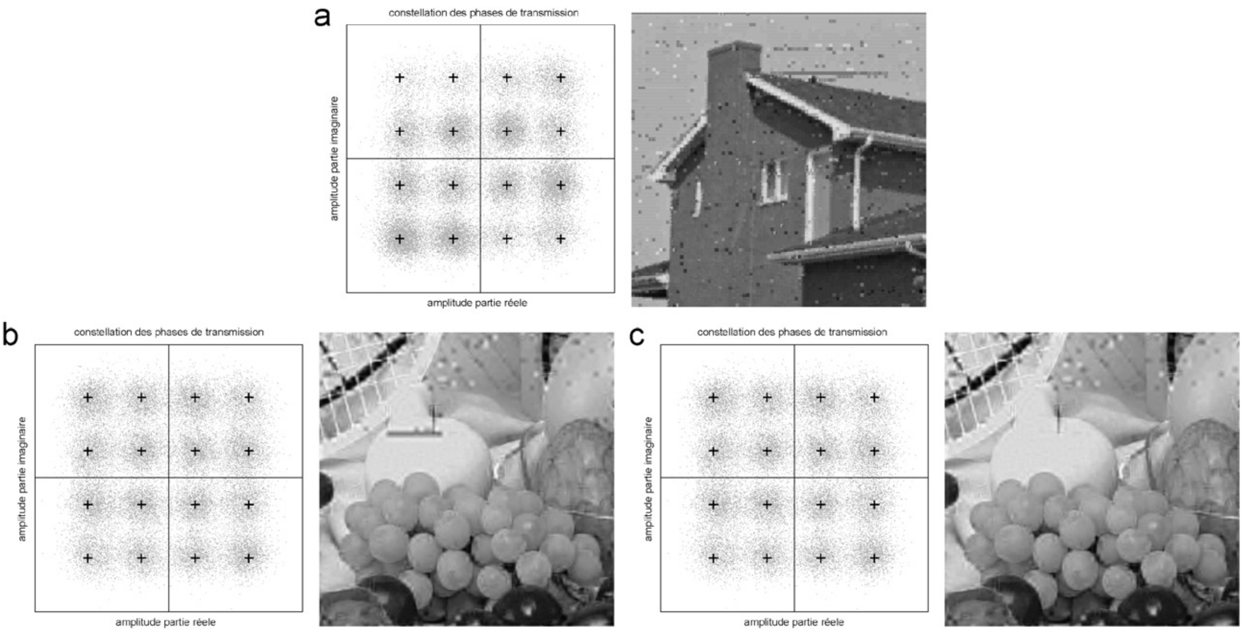

Fig. 15. Received images after transmission over the ionospheric channel and 16-QAM associated constellations. (a) SOM image + RS(255,227) code, BER = 1.69 10^{-2}, soft decoding; (b) WTSOM image + RS(255,187) code, BER = 1.66 10^{-2}, hard decoding; (c) WTSOM image + RS(255,187) code, BER = 1.66 10^{-2}, soft decoding.

The results show the advantage of the WTSOM method, which uses a hierarchical protection of the data compared with the SOM method. Even with hard decoding, the visual quality is good enough for video conference applications when the BER is very high (1.6×10^{-2}). However the issue of the operational image quality remains. The PSNR criterion currently used is limited, i.e., the absolute value of a PSNR does not guarantee an image without visually significant artefacts. We therefore propose a parameter called $\mathrm{PSNR}_{\%}$, which allows calculating the proportion of PSNR loss between the transmitter and the receiver in a transmission chain. If $\mathrm{PSNR}_{\mathrm{T}}$ is the PSNR value of the compressed image at the transmitter and $\mathrm{PSNR}_{\mathrm{R}}$ is the PSNR of the received image, then $\mathrm{PSNR}_{\%}$ can be calculated with

$$\begin{aligned}\mathrm{PSNR}_{\%} &= 100 - 100\left(\frac{\mathrm{PSNR}_{\mathrm{T}} - \mathrm{PSNR}_{\mathrm{R}}}{\mathrm{PSNR}_{\mathrm{T}}}\right)\\ &= 100\frac{\mathrm{PSNR}_{\mathrm{R}}}{\mathrm{PSNR}_{\mathrm{T}}}.\end{aligned} \quad (3)$$

Because of the characteristics of the ionospheric channel, it is impossible to obtain the same values of SNR and BER from one image transmission to another. Fig. 16 shows a synthesis of different results for the coding and decoding schemes presented in this paper. The following figure presents the $\mathrm{PSNR}_{\%}$ as a function of the BER and highlights that WTSOM associated with soft decoding is consistently better than all other methods.

These results can be compared with those presented in Fig. 17.

They were published in [9] and are related to JPEG 2000 WireLess (JPWL) transmission over a binary symmetric channel. In order to obtain these results, the authors used UEP and EEP with different RS codes yielding an overall code rate of 2/3. Using our PSNR% criterion and assuming that PSNR_T = 32 dB and PSNR_R = 27 dB at a BER = 10^{-2} for the JPWL encoded image, we obtained PSNR_% = 84% in the UEP case. In the WTSOM case, for the same BER we obtain PSNR_% = 97% for a much lower code rate (0.9). However, we must be very careful with such a conclusion since we do not have the same transmission conditions and not the same channel.

6. Conclusion

In this paper, we have presented a robust JSCC scheme for image transmission over the ionospheric channel. Our scheme is based on a DWT, a VQ optimally mapped on digital modulations and an UEP of the information. In our application, this scheme is especially dedicated to low bit rate and

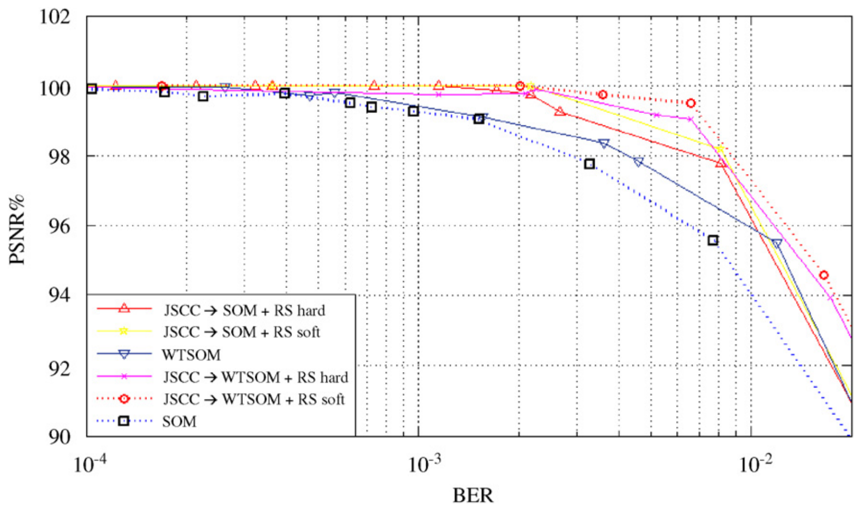

Fig. 16. PSNR% as a function of BER for several configurations and coding strategies.

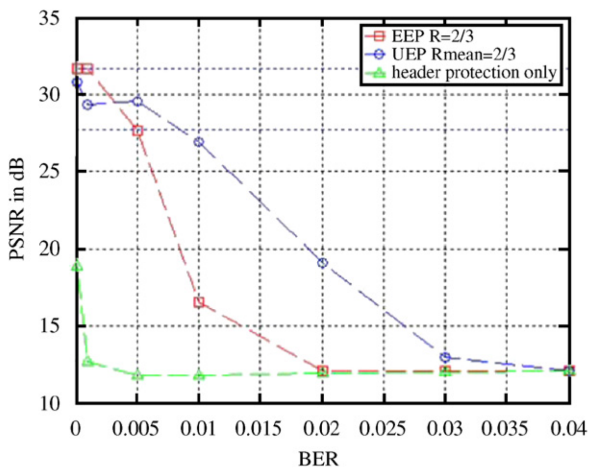

Fig. 17. PSNR results for UEP and EEP on "Woman" image [28].

high BER channels such as the ionospheric channel. We have shown that our approach gives better results than the usual associations between VQ and QAM techniques for the same compression rate without a great complexity increase. The use of a Reed-Solomon code to protect the most important data allows decreasing the distortion of the reconstructed image, when a soft decoding stage is implemented. Indeed we propose a criterion called $PSNR_{\%}$, which calculates the PSNR loss between the transmitter and the receiver in a transmission chain. This coding scheme was tested on an operational radio link over the ionospheric channel and the experimental results confirmed the robustness of the wavelet transform self-organizing map strategy even for very bad conditions of transmission.

Acknowledgements

We would like to thank Mrs. Irène Richardson for her help during the writing of the paper and the anonymous reviewers for their helpful comments to improve the quality of this paper.

References

[1] M. Antonini, M. Barlaud, P. Mathieu, I. Daubechies, Image coding using wavelet transform, IEEE Trans. Image Process. 1 (2) (1992) 205–220.
[2] A. Bisiaux, L. Bertel, C. Barratt, D. Lemur, Trilion Project: Transmission of Images Through Ionophere, IEE, H.F. Radio Systems and Techniques, July 2000, Guilford, UK, pp. 1–5.
[3] K.G. Budden, The Magneto-Ionic Theory and its Applications to the Ionosphere, Cambridge University Press, Cambridge, 1985.
[4] R.M. Capocelli, A.A. De Santis, L. Gargano, U. Vaccaro, On the construction of statistically synchronizable codes, IEEE Trans. Inform. Theory 38 (2) (March 1992) 407–414.
[5] D. Chase, A class of algorithms for decoding block codes with channel measurement information, IEEE Trans. Inform. Theory 18 (1) (1972) 170–182.
[6] P.C. Cosman, J.K. Rogers, P.G. Sherwood, K. Zeger, Combine forward error control and packetized zerotree wavelet encoding for transmission of images over varying channels, IEEE Trans. Image Process. 9 (6) (2000) 982–993.
[7] V. DeBrunner, L. DeBrunner, L. Wang, S. Radhakrishan, Error control and concealment for image transmission, IEEE Commun. Soc. Surveys Tutor. 3 (1) (2000) 2–9.
[8] F. Dufaux, G. Baruffa, F. Frescura, D. Nicholson, JPWL-an extension of JPEG 2000 for wireless imaging, in: Proceeding

of International Symposium on Circuits and Systems, 21–24 May 2006.
[9] Y. Erhel, C. Perrine, C. Chatellier, D. Lemur, P. Bourdon, High data rate, radiocom-munications through the ionospheric channel, Elsevier/Int J. Electron. Commun. 61 (4) (2006) 270–278.
[10] T. Ferguson, J. Rabinowitz, Self synchronizing Huffman codes, IEEE Trans. Inform. Theory 30 (4) (1984) 687–693.
[11] E.W. Forgy, Cluster analysis of multivariate data: efficiency versus interpretability of classification, Biometrics 21 (3) (1965) 768–769.
[12] R.M. Gray, Vector quantization, IEEE Acous. Speech Signal Process. Mag. 1 (2) (1984) 4–29.
[13] J. Kangas, in: Increasing the error tolerance in transmission of vector quantize image by self organizing map, International Conference on Artificial Neural Networks, vol. 1, Paris, 1995, pp. 287–291.
[14] IEEE 78 (9) (1990) 1464–1480.
[15] T. Kohonen, Self Organization and Associative Memory, second ed., Springer, Berlin, 1994.
[16] W.M. Lam, A. Reibman, Self-synchronization variable length codes for image transmission, in: IEEE International Conference on Acoustics Speech and Signal Processing, vol. 3, San Francisco, California (USA), March 1992, pp. 477–480.
[17] J. Mac Queen, Some methods for classifications and analysis of multivariate observations, in: Fifth Berkeley Symposium on Mathematical Statistics and Probability, vol. 1, University of California Press, Berkeley, 1967, pp. 281–297.
[18] W. Pennebaker, J. Mitchell, The JPEG still Image Data Compression Standard, Kluwer Academic Publisher, Van Nostrand Reinhold, December 1992.
[19] C. Perrine, Y. Erhel, D. Lemur, L. Bertel, A. Bourdillon, A way to increase the bit rate in ionospheric radio links, Ann. Geophys. 47 (2004) 1145–1160.
[20] R. Pyndiah, B. Solaiman, O. Aitsab, Optimized source coding and coded modulation for digital transmission of still images on a noisy channel, IEEE Intl. Conf. Image Process. 2 (1998) 142–146.
[21] I.S. Reed, G. Solomon, Polynomial codes over certain finite fields, J. Soc. Ind. Appl. Math. 8 (2) (1960) 300–304.
[22] A. Said, W. Pearlman, A new, fast, and efficient image codec based on set partitioning in hierarchical trees, IEEE Trans. Circ. Systems Video Technol. 6 (3) (1996) 243–250.
[23] S. Salous, L. Bertel, Modelling of wideband HF radio channels, in: International Conference on Antennas and Propagation, Davos, 2000, pp. 1–4.
[24] P.G. Sherwood, K. Zeger, Error protection for progressive image transmission over memoryless and fading channels, IEEE Trans. Commun. 46 (12) (1998) 1555–1559.
[25] B. Souhard, C. Chatellier, C. Olivier, On the robustness of joint source/channel coding for transmission through an ionospheric channel, HF2003, IEE Ninth International Conference on HF Radio Systems and Techniques, University of Bath, UK, Juin 2003, pp. 108–113.
[26] D. Taubman, High performance scalable image compression with EBCOT, IEEE Trans. Image Proces. 9 (7) (2000) 1158–1170.
[27] D. Taubman, M. Marcellin, JPEG2000: Image Compression Fundamental Standards and Practice, Kluwer Academic Publisher, Dordrecht, 2001.
[28] IEEE Trans. Image Process. 15 (1) (2006) 54–67.

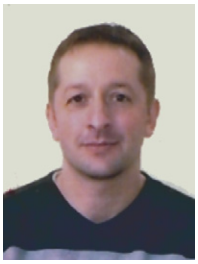

Christian Chatellier received his M.S. degree in electronics in 1989 and his Ph. D. in electronics and signal treatments in 1993 from Poitiers University, France. In 1994, he joined the Signal Image Communication Laboratory as an Associate Professor in this University. His research interests are mainly Digital Communication Systems and joint source/channel coding schemes for image transmission over wireless channels.

Hervé Boeglen received the M.S. degree in electrical engineering from the University of Haute-Alsace, Mulhouse, France in 2004. He is currently working toward the Ph.D. degree in electrical engineering. His research interests are in digital communications with an emphasis on mobile communications and channel modeling.

Clency Perrine received his M.S. degree in telecommunications in 2002 and his Ph.D. in telecommunications and signal processing in 2005 from the University of Rennes 1. His thesis deals with an operational system for images transmission in HF band (3–30 MHz). In September 2006, he joined the SIC laboratory in Poitiers as an associate professor. His research interests are focused on Digital Communication Systems and joint source/channel coding schemes for images transmission through non-stationary wireless channels.

Christian Olivier received the degree in Mathematics (Signal Processing) in 1979. His major interest was in stochastic process modelling. He was an Associate Professor at the University of Rouen from 1987 to 1997 where his research area was mathematical tools for image segmentation, pattern analysis and recognition. Then he joined the University of Poitiers as a Professor. His research is now information representation, especially for image coding and wireless transmission (source-channel coding).

Olivier Haeberlé is Professor at University of Haute-Alsace (Mulhouse-France) in electrical engineering and computer sciences. Since 1998 at Modelisation Intelligence Process and Systems (MIPS) Laboratory, his work focuses on 3-D fluorescence microscopy, and 3-D tomographic diffractive microscopy, with emphasis in image formation modeling, and image processing (deconvolution, denoising) and reconstruction.